Endoglin-targeted contrast-enhanced ultrasound imaging in hepatoblastoma xenografts

RONG SHAN[1,2], BEI WANG[3], AIGUANG WANG[4], ZONGGUO SUN[5], FENGYUN DONG[5], JU LIU[5] and HONGJUN SUN[3]

[1]Department of Ultrasonography, Jinan Infectious Disease Hospital, Jinan, Shandong 250021; [2]Department of Ultrasound, Shandong University, Jinan; Departments of [3]Ultrasonography and [4]Oncology; [5]The Medical Research Center, Shandong Provincial Qianfoshan Hospital, Shandong University, Jinan, Shandong 250014, P.R. China

Received December 12, 2016; Accepted June 4, 2018

DOI: 10.3892/ol.2018.9067

Abstract. Angiogenesis is required for the growth of hepatoblastoma (HB). In the present study, an ultrasonic contrast agent, microbubbles (MB), was combined with an endoglin antibody, and then injected into nude mice with HB. This was conducted to detect specific binding to microvessels via non-linear harmonic imaging for tumor angiogenesis assessment. In addition, endoglin expression in experimental animals was measured using western blotting, reverse transcription-quantitative polymerase chain reaction and immunohistochemistry. *In vitro*, human umbilical vein endothelial cells (HUVECs) were co-cultured with conditioned media collected from HepG2 cells. Western blotting and reverse transcription-quantitative PCR was performed to detect the changes of endoglin expression. In targeted ultrasound imaging, it was determined that the differential targeted enhancement of $MB_{endoglin}$ was significantly higher than that of $MB_{isotype}$. Over expression of endoglin was identified in the tumor of experimental nude mice; however, it was not present in the liver of the mice. Endoglin expression in HUVECs was significantly increased by co-culture with the conditioned media of HepG2 cells; therefore, the results suggest that endoglin is upregulated in angiogenic vessels in the HepG2 cell xenografts in nude mice. Thus, endoglin-targeted ultrasound imaging is presented as a potential approach for the diagnosis of liver carcinoma.

Correspondence to: Professor Hongjun Sun, Department of Ultrasonography, Shandong Provincial Qianfoshan Hospital, Shandong University, 16766 Jingshi Road, Jinan, Shandong 250014, P.R. China
E-mail: sunhongjunqy@163.com

Professor Ju Liu, The Medical Research Center, Shandong Provincial Qianfoshan Hospital, Shandong University, 16766 Jingshi Road, Jinan, Shandong 250014, P.R. China
E-mail: ju.liu@sdu.edu.cn

Abbreviations: HB, hepatoblastoma; MB, microbubbles; HUVECs, human umbilical vein endothelial cells; VEGFR2, vascular endothelial growth factor receptor 2; RT-qPCR, reverse transcription-quantitative polymerase chain reaction

Key words: endoglin, microbubbles, hepatoblastoma angiogenesis, ultrasound imaging

Introduction

Hepatoblastoma (HB) is an aggressive type of cancer that has a high morbidity and mortality rate in children (1). Early diagnosis and treatment are important for improving the survival rate of patients with HB. The majority of HBs are hypervascular (2); therefore, angiogenesis may serve a vital role in HB development and metastasis. Angiogenesis is the formation of new blood vessels, and is a hallmark of early-stage tumors (3). The growth of solid tumors relies on neovascularization (4). Tumor and endothelial cells may constitute a highly integrated system, which could cause a mutual growth promotion (5,6). Tumor cells secrete specific cytokines to stimulate the proliferation of vascular endothelial cells, and the endothelial cells may modulate tumor cell growth by providing oxygen and nutrients (6). During angiogenesis, specific molecular markers are overexpressed on the surface of endothelial cells (3).

Endoglin, also termed CD105, is a homodimeric transmembrane glycoprotein that contains 561 amino acid residues in its extracellular domain and 47 amino acids in a cytoplasmic tail domain (7). It is a major component of the transforming growth factor-β (TGF-β) receptor complex (8). Endoglin is expressed in adult vascular endothelial cells and stromal cells (7). In cultured endothelial cells, higher levels of endoglin expression can be detected during proliferation (9). In tumor tissues, endoglin is overexpressed during remodeling in angiogenic vessels (10); therefore, endoglin is a biomarker for angiogenesis (11-13). A previous study identified that endoglin was expressed in 100% of surgically resected specimens, in both tumor tissues and para-carcinomatous tissues (14).

Recently, ultrasound molecular imaging has emerged as a means of visualizing disease processes at the molecular level *in vivo*. This technique has the ability to qualitatively and quantitatively illustrate specific molecules in tissues, cells or subcellular organelles. With the development of targeted ultrasound contrast agents, ultrasound has the ability to detect molecular changes in living cells. The targeted

microbubbles (MB), ranging in size from 1-4 μm (15), usually consist of an insoluble gas, including perfluoropropane, perfluorobutane, perfluorohexane, or sulfur hexafluoride and the bubble's outer wall (16). The ligands (antibody, peptide and scaffold) were bound to the shell by covalent or non-covalent bonding (17). Following intravenous injection, targeted MB bound to specific molecules in the circulatory system (Fig. 1).

The vibrations of the MB compression and expansion may be distinguished with background noise under the non-linear contrast ultrasonic mode (18,19). Pre-clinical studies demonstrated that molecular ultrasound imaging may detect angiogenesis in tumors (20-23). Deshpande *et al* (24) assessed three types of molecular-targeted ultrasound MB: $MB_{integrin}$, $MB_{endoglin}$ and MB_{VEGFR2} in animal models with three subcutaneous cancer xenografts (breast, ovarian and pancreatic cancer). Their results indicated a significantly higher expression of endoglin than αvβ3 integrin and VEGFR2 expression in early stage breast and ovarian cancers.

In the present study, MB and endoglin were combined and injected into nude mice with HB to measure specific binding to microvessels, for the purpose of tumor angiogenesis diagnosis via non-linear harmonic imaging. In addition, the techniques used to detect endoglin expression in experimental animals included western blotting, reverse transcription-quantitative polymerase chain reaction (RT-qPCR), and immunohistochemistry. Conditioned medium of HB cells was applied to incubate human umbilical vein endothelial cells (HUVECs) to detect changes of endoglin expression in HUVECs.

Materials and methods

Experimental model. All the animals in the present study were provided by Professor Yourong Duan from the Shanghai Cancer Institute (Shanghai, China). HepG2 cells were cultured in Dulbecco's modified Eagle's medium (DMEM) supplemented with 10% fetal bovine serum (FBS; Lonza Group, Ltd., Basel, Switzerland) and 1% antibiotics (100 IU/ml penicillin and 100 μg/ml streptomycin; Sigma-Aldrich; Merck KGaA, Darmstadt, Germany). Four BALB/c male nude mice, which were 3-4 weeks old and weighing 22-25 g, were used in the present study and maintained in a pathogen-free environment. Mice were maintained in standard transparent polycarbonate cages and fed with Food pellets (Lab Diet 5010; LabDiet, Richmond, IN, USA) with water. The room was maintained with clean atmosphere, the lighting on a 12 h light/dark cycle, and the room temperature between 20˚C and 22˚C. Allograft tumors were produced via a subcutaneous injection of $5x10^6$ HepG2 cells suspended in 0.2 ml sterile PBS into the right flank of the nude mice. After three weeks, the maximum diameter of the tumors was 0.5 cm, which was suitable for molecular ultrasound imaging.

Molecular ultrasound imaging. The *in vivo* distribution of the isotype and endoglin-targeted MB was examined in mice with the HepG2 subcutaneous tumors (n=4) by the Vevo® 2100 small animal high-resolution ultrasound system with the MS-250 transducer (VisualSonics, Inc., Toronto, ON, Canada). The frequency of the transducer is 40 MHz. Isotype and targeted MB were prepared using Vevo® MicroMarker® Target-Ready Contrast Agent kits (VisualSonics, Inc.). Biotinylated anti-endoglin and isotype anti-mouse-IgG antibodies were purchased from Abcam (Cambridge, MA, USA). The MB were prepared according to the manufacturer's instructions, and the ultrasound system was operated using The Guide to Small Animal Nonlinear Contrast Imaging (25). Capturing ultrasound imaging was completed following the intravenous injection of $5x10^7$ $MB_{Isotype}$ through the tail vein and followed by sequence destruction. $MB_{endoglin}$ ($5x10^7$) was injected 30 min after the isotype was cleared from circulation. The echo intensity prior to the destruction pulse represents bound/circulating microbubbles and tissue signal. The echo intensity following the destruction pulse represents the microbubbles that are still in circulation and the residual tissue-echoes, not the binding process. In the Targeted model, Vevo Contrast Quantification (Vevo CQ™) Software (version 1.3.12.0; VisualSonics, Inc, Toronto, Ontario, Canada.) is able to express the specific binding as a difference between the echo power averaged in the segment before destruction pulse and the residual echo power averaged in the segment after destruction pulse. The Vevo CQ™ Software was used to visualize the spatial distribution of perfusion parameters as color-coded parametric images. The differential targeted enhancement (ΔTE) was computed by subtracting the mean intensity detected after the destructive pulse from the mean intensity detected prior to the destructive pulse. Liver and tumor tissues were isolated for examination by immunohistochemistry, western blotting and RT-qPCR.

RT-qPCR. Total RNA was isolated from cultured cells, and the liver and tumor tissues of nude mice, using TRIzol® reagent (Invitrogen; Thermo Fisher Scientific, Inc., Waltham, MA, USA). RNA isolation and cDNA synthesis were performed using an RNeasy Mini kit (Qiagen GmbH, Hilden, Germany) and the High Capacity RNA-to-cDNA Master Mix (Applied Biosystems; Thermo Fisher Scientific, Inc.) RT-qPCR was performed with a ViiA7 Real-Time PCR System (Applied Biosystems; Thermo Fisher Scientific, Inc.) and using SYBR-Green Master Mix (Thermo Fisher Scientific, Inc.). An aliquot of 2 μg total RNA from each sample was used for the synthesis of cDNA using a High-Capacity cDNA Reverse Transcription kit (Applied Biosystems; Thermo Fisher Scientific, Inc.). cDNA was amplified in a final volume of 20 μl with 1 U Taq DNA polymerase (Invitrogen; Thermo Fisher Scientific, Inc.) and 10 pmol of each primer. Reaction conditions were as follows: 95˚C for 5 min, 40 cycles of 95˚C for 10 sec and 60˚C for 32 sec. All PCR reactions were conducted in triplicate. Relative expression was calculated by comparing the relative expression level of CD105 with the internal reference GAPDH by the $2^{-\Delta\Delta Ct}$ method (26). Primer sequences are listed in Table I.

Western blot analysis. Western blotting was performed as previous described (27). Briefly, cells were lysed in ice-cold RIPA buffer (20 mM Tris pH 7.5, 150 mM NaCl, 50 mM NaF, 1% NP40, 0.1% DOC, 0.1% SDS, 1 mM EDTA and supplemented with 1 mM PMSF and 1 μg/ml leupeptin). Equal amounts of protein (40 μg), as determined by a BCA assay, were separated via 10% SDS-PAGE and then transferred to a polyvinylidene fluoride membrane. Membranes were blocked with 2.5% non-fat milk and incubated with an rabbit polyclonal

Table I. RT-qPCR primer sequences.

Gene	Sequence	Product size (bp)	TM (˚C)
CD105-mouse			
Forward	5'-CCCTCTGCCCATTACCCTG-3'	11	59.5
Reverse	5'-GTAAACGTCACCTCACCCCTT-3'	7	57.6
CD105-human			
Forward	5'-CGCCAACCACAACATGCAG-3'	15	57.3
Reverse	5'-GCTCCACGAAGGATGCCAC-3'	8	59.5
GAPDH-mouse			
Forward	5'-AAGGATGAAGGAAGTGATTTG-3'	40	53.77
Reverse	5'-AAGAGGAACATCGTGGTAAAG-3'	3	55.62
GAPDH-human			
Forward	5'-TGATGACATCAAGAAGGTGGTGAAG-3'	24	61.03
Reverse	5'-TCCTTGGAGGCCATGTGGGCCAT-3'	0	68.32

Bp, base pair; Tm, temperature; RT-qPCR, reverse transcription-quantitative polymerase chain reaction; GADPH, glyceraldehyde-3-phosphate dehydrogenase.

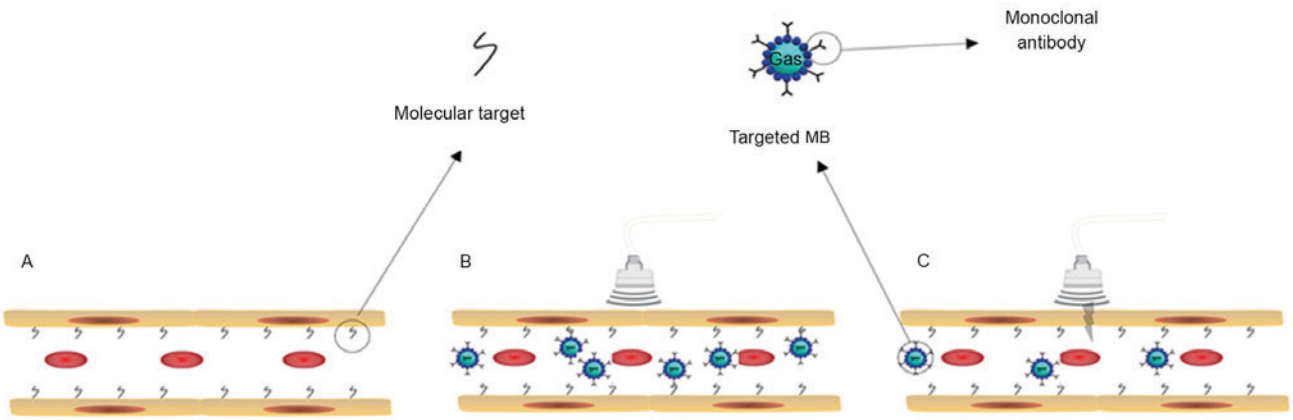

Figure 1. Illustration of microbubble-targeted ultrasound imaging. (A) Prior to MB injection. (B) After injection, bound and freely circulating MB can be imaged by ultrasound. (C) A sequence destruction pulse destroys all MB (bound and circulating) in the imaging plane. Following the pulse, remaining circulating MB re-circulated into the imaging plane; therefore, the intensity change represents the extent of bound MB. MB, microbubbles.

anti-CD105 antibody (dilution 1:400; cat. no. ab107595; Abcam, Cambridge, MA, USA) in PBS with Tween 20 (TBST) at 4˚C overnight. Subsequent to washing with TBST 3 times, the membrane was incubated with the secondary antibody at 37˚C for 1 h. The secondary antibody was horseradish peroxidase-conjugated anti-rabbit IgG (dilution 1:6,000; cat. no. SA00001-2; Protein Tech Group, Inc.; Wuhan Sanying Biotechnology, Wuhan, China). The membranes were then visualized with an enhanced chemiluminescence reagent (cat. no. WBKLS0500; Merck KGaA).

Immunohistochemical staining. Tissue preparation and immunohistochemistry was performed as previously described (28). Briefly, 6 μm serial sections were cut from the blocks of each mouse liver or tumor. The slides were deparaffinized in xylene and rehydrated in gradient ethyl alcohol of 100, 95, 85, 80 and 75%. Antigen retrieval was performed in a citrate salt antigen repair solution for 15 min in a pressure cooker at 120˚C, then the sections were cooled to room temperature and washed with PBS three times. Sections were incubated with rabbit anti-mouse CD105 polyclonal antibody (dilution 1:50; cat. no. ab107595; Abcam, Cambridge, UK) at 4˚C overnight. Then the sections were placed in room temperature for 40 min, washed with PBS three times and incubated with biotinylated rabbit anti-rat IgG (dilution 1:500; cat. no. BA4000; Vector Laboratories, Inc., Burlingame, CA, USA) at 37˚C for 20 min. The sections were incubated with 20X DAB substrate buffer (cat. no. ZLI-9017; Origene Technologies, Inc., Beijing, China) for 1 min. The slides were then counterstained with hematoxylin (Surgipath®; Leica Microsystems GmbH, Wetzlar, Germany) at room temperature for 1 min and dehydrated through five grades of alcohol (75, 80, 95 and 100%) and xylene. The slides were observed under a light microscope and images were captured with an Olympus FSX100 imaging system (Olympus Corporation, Tokyo, Japan) and analyzed by Image Pro Plus 6.0 software (Media Cybernetics, Inc., Rockville, MD, USA) (magnification, x400).

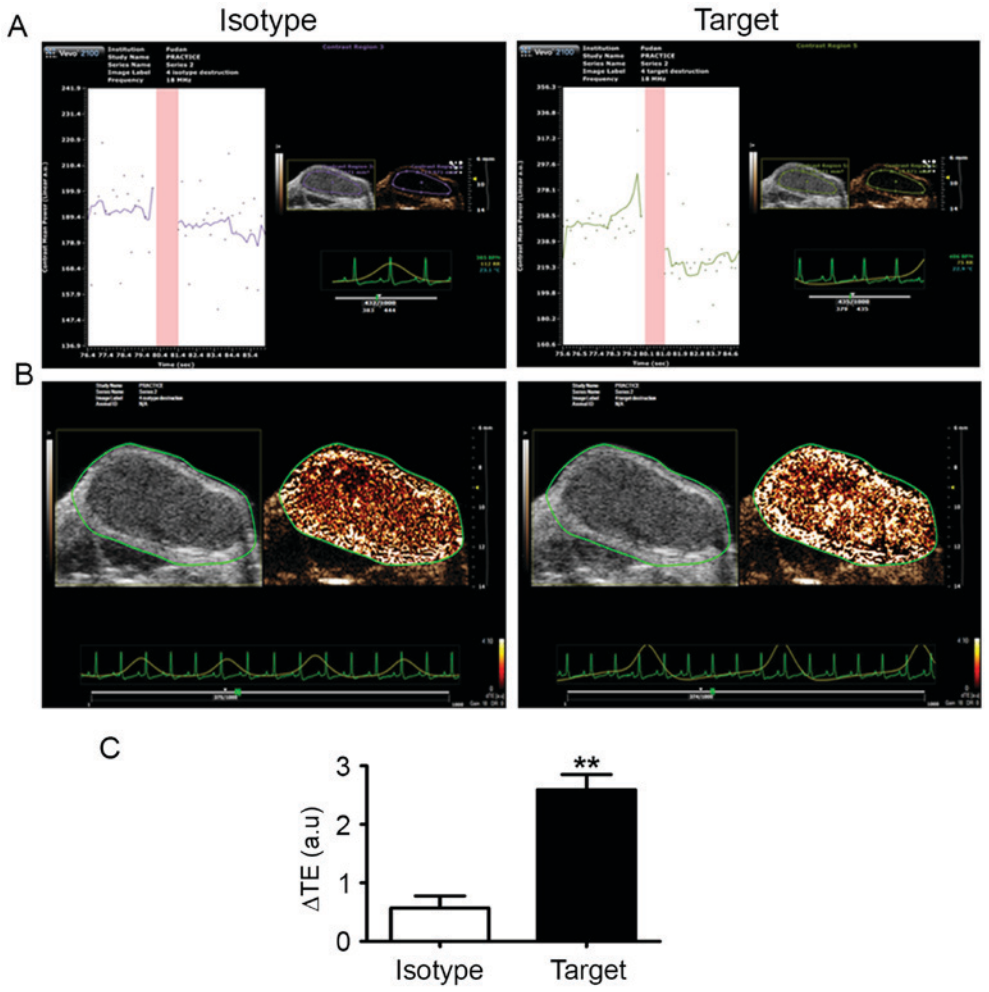

Figure 2. Isotype and endoglin-targeted ultrasound molecular imaging of a nude mouse with subcutaneous HB. (A) Intensity graph for the traced regions of interest prior to and after the destruction pulse (pink region). The region on the left of the column is prior to destruction, and on the right of it is after destruction. The change in intensity following the destruction pulse is an index of the amount of specific binding. The linearized signal prior to the destruction pulse represents bound and circulating microbubbles (MB) and tissue signal. The linearized signal after the destruction pulse corresponds to the MB that were still in circulation and to any residual tissue-echoes, and does not represent the binding process. The ΔTE was computed by subtracting the mean intensity detected after the destructive pulse from that prior to the destructive pulse. (B) Parametric imaging. The scale bar of ΔTE is on the right corner of the map. (C) ΔTE of isotype and endoglin-targeted MB. $\Delta TE = TE_{fd} - TE_{pd}$. n=4; $^{**}P<0.001$. TE, targeted enhancement; ΔTE, differential TE; fd, following destruction; pd, prior to destruction; MB, microbubbles.

Conditioned medium cell culture. The human HB carcinoma cell line HepG2 and human umbilical vein endothelial cells (HUVECs) purchased from American Type Culture Collection (Manassas, VA, USA), were cultured in DMEM supplemented with 10% FBS, 100 IU/ml penicillin and 100 μg/ml streptomycin. All the cells were maintained at 37˚C in a humidified atmosphere containing of 5% CO_2. HepG2 cells were incubated with DMEM, containing 0.5% FBS, 100 IU/ml penicillin and 100 μg/ml streptomycin, and the conditioned media was collected after 12 h. HUVECs were co-cultured with conditioned media from HepG2 cells. The cells were lysed with TRIzol reagent (Invitrogen; Thermo Fisher Scientific, Inc.). The total mRNA and protein was collected for western blotting and RT-qPCR detection after 12 h.

Statistical analyses. Statistical significance was assessed using paired-sample student's t-tests. All statistical analyses were performed using SPSS 17.0 statistical software (SPSS Inc., Chicago, IL, USA). P<0.05 was considered to indicate a statistically significant difference.

Results

Targeted ultrasound imaging. The experimental animals were tolerant of ultrasound contrast imaging, with no acute toxic reactions observed. To confirm the specific binding of $MB_{endoglin}$, $MB_{isotype}$ was injected to eliminate non-specific binding. Following ultrasound imaging capturing, the ΔTE of $MB_{endoglin}$ and $MB_{isotype}$ was calculated automatically using the built-in software (VisualSonics, Inc.). Previous studies demonstrated that endoglin is an excellent biomarker of angiogenesis (9-13). In the present study, anti-endoglin monoclonal antibodies were bound to MB to target overexpressed endoglin on the surface of tumor vessel endothelial cells in subcutaneous HepG2 xenografts in nude mice. The echo intensity taken prior to the destruction pulse represent bound and circulating MB, and the tissue signal. The echo intensity following the destruction pulse correspond to MB that remained in circulation and to any residual tissue-echoes, which are not representative of the binding process. The difference between prior to and following destruction is the intensity of bound MB. The ΔTE of

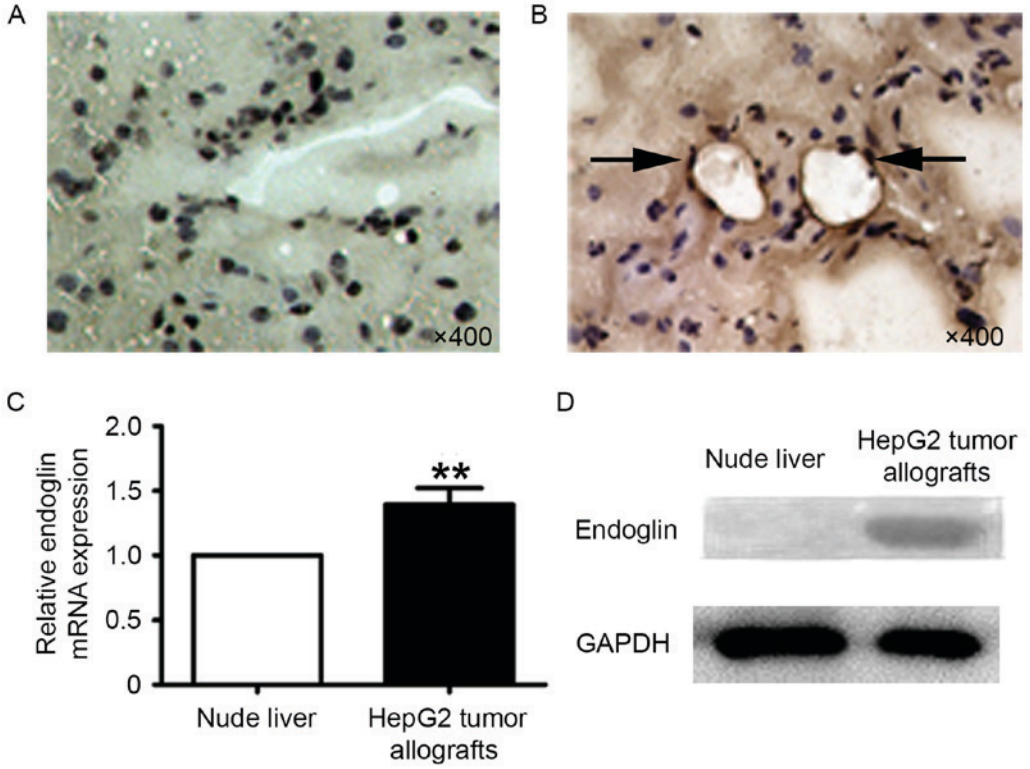

Figure 3. Endoglin expression in the livers of nude mice and HepG2 tumor xenografts. Western blot analysis of endoglin antibody binding in (A) the liver tissues of nude mice and (B) HepG2 cell xenografts of nude mice. The arrows refer to positively stained blood vessels. Original magnification, x40. (C) Relative endoglin mRNA expression. n=4; **P<0.001; (D) Representative western blotting of endoglin and glyceraldehyde-3-phosphate dehydrogenase. GAPDH, glyceraldehyde-3-phosphate dehydrogenase.

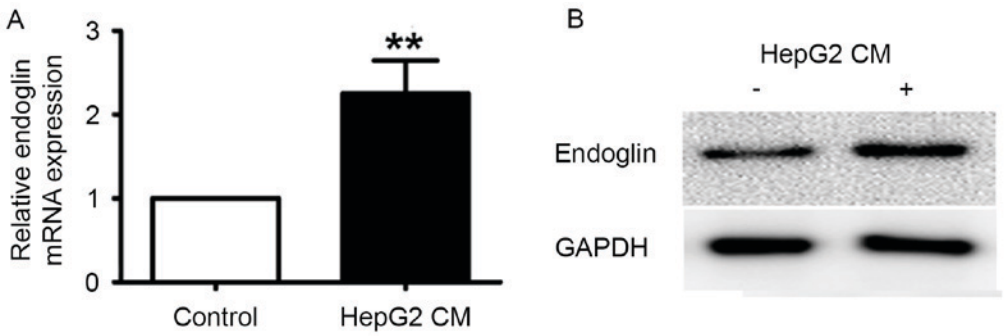

Figure 4. Endoglin expression in HUVECs treated with the CM of HepG2 cells. (A) Relative endoglin mRNA expression and (B) representative western blotting of HUVEC samples treated with control media and CM from HepG2 cells. n=4; **P<0.001. CM, conditioned media; HUVECs, human umbilical vein endothelial cells.

$MB_{endoglin}$ was higher than that of $MB_{isotype}$ (Fig. 2A and B), with the difference being statistically significant (P<0.001; Fig. 2C).

Endoglin expression in the liver tissues and HepG2 tumor allografts of nude mice. Tissues extracted from experimental nude mice liver and subcutaneously allografted HepG2 tumors underwent immunohistochemical staining, RT-qPCR analysis and western blot analysis. Endoglin is not expressed on the endothelium of microvessels in the normal liver tissue and blood vessels (Fig. 3A), but is expressed in the HepG2 tumors (Fig. 3B, as the black arrow indicates). RT-qPCR analysis demonstrated that endoglin mRNA expression in the HepG2 tumors was significantly higher than in the liver tissues of the nude mice (n=4; P<0.001; Fig. 3C). Western blot analysis was performed to evaluate endoglin expression. Endoglin was present in the protein extracts of HepG2 tumors; however, it was absent in the liver tissues of nude mice (Fig. 3D).

Endoglin expression in HUVECs treated with the conditioned media of HepG2 cells. In cultured endothelial cells *in vitro*, high endoglin expression could be detected in the cells during proliferation and activation. To mimic the microenvironment of tumor vessels, conditioned media from HepG2 cells were collected and applied to HUVECs. Following culturing in HepG2-conditioned media for 12 h, endoglin mRNA levels were significantly upregulated in HUVECs (P<0.001; Fig. 4A). Protein extracts of HUVECs were also collected for examination of protein expression by western blotting.

As depicted in Fig. 4B, endoglin protein levels were significantly greater in HUVECs treated with HepG2-conditioned media ($P<0.001$).

Discussion

The growth of HB is dependent on angiogenesis, which is stimulated by vaso-active substances from HB cells (29). Blood supply to liver tumors is from the hepatic artery and forms disordered nourishing vessels (30). In the present study, MB were bound to an anti-endoglin antibody, and then injected into HB xenograft tissues in nude mice in order to detect specific binding to tumor microvasculature, via non-linear harmonic imaging. It was determined that the ΔTE of $MB_{endoglin}$ was significantly higher than that of $MB_{isotype}$. In addition, increased expression of endoglin was identified in the HB xenografts, but not in the livers of recipient nude mice. *In vitro*, treatment with the conditioned media of HepG2 cells increased endoglin expression in HUVECs; therefore, endoglin is specifically overexpressed in HB vascular endothelial cells, which can be detected by endoglin-bound MB.

In the past ten years, a novel technique for ultrasound has been utilized for molecular imaging, which visualizes disease processes at the molecular level at target locations (25,31). With the introduction of a novel targeted ultrasound contrast agent, disease processes could be visualized at molecular level qualitatively and quantitatively (18). Currently, the most widely used ultrasound contrast agents are MB designed in micrometers to detect and monitor the expression of molecules on the endothelium (32,33). Targeted enhanced-contrast ultrasound could improve the detection rate of early-stage HB by the specific targeted combination of MB concentrating on tumor angiogenesis.

Several newly discovered angiogenesis markers, including VEGFR2 and CD34, were verified by molecular ultrasound imaging *in vivo* (25,34-36). Endoglin is overexpressed in angiogenic endothelial cells of various tumors (12,33,35,37). It is part of the TGF-β receptor complex (11-13). Interaction of endoglin with activated activin receptor-like kinase 1 (ALK1), ALK5 and TGF-β Receptor 2 results in phosphorylation of serine and threonine residues in the cytoplasmic domain of endoglin (36). ALK1 is exclusively expressed in endothelial cells and induces the phosphorylation of endoglin, which regulates endothelial cell proliferation (36). In the present study, it was demonstrated that endoglin is overexpressed in vasculature in HB xenografts and endoglin expression can be upregulated by co-culture with HB cells. In addition, endoglin-antibody-bound MB to detect angiogenic vessels in HB xenografts in nude mice were successfully used. Ultrasound molecular imaging is particularly valuable in early detection, differentiation of focal lesions and treatment monitoring. Several biomarkers in ultrasound molecular imaging have been reported for detecting early-stage tumors (37). Endoglin could be considered a novel marker for early-stage tumors detectable via targeted ultrasound imaging.

To summarize, it was demonstrated that endoglin-targeted ultrasound imaging recognizes subcutaneous HepG2 xenografts in nude mice, and that endoglin expression in endothelial cells is upregulated by co-culture with HepG2 cells *in vitro*.

In conclusion, endoglin is upregulated in angiogenic vessels in HepG2 cell xenografts in nude mice. Endoglin-targeted ultrasound imaging has been verified as a potential novel method for the diagnosis of liver carcinoma.

Acknowledgements

The authors are grateful for the support from the Shandong Taishan Scholarship (Professor Ju Liu, Shandong University, Jinan, China).

Funding

The present study was supported by the grants from the Science and Technology Development Plan of Shandong Province (grant no. 2014GSF118062), the Special Research Program for Public Services of Shandong Province (grant no. 2014fwyyd04).

Availability of data and materials

The datasets generated and analyzed in the present study are available from the corresponding author upon reasonable request.

Authors' contributions

JL, RS and HS conceived and designed the experiments; RS, BW, FD, AW, ZS performed the experiments; JL, RS, HS analyzed the data; JL, RS, HS wrote the paper.

Ethics approval and consent to participate

The procedures in the present study were approved by the ethics committee of Shandong Provincial Qianfoshan Hospital (Jinan, China).

Patient consent for publication

Not applicable.

Competing interests

The authors declare that they have no competing interests.

References

1. Tomlinson GE and Kappler R: Genetics and epigenetics of hepatoblastoma. Pediatr Blood Cancer 59: 785-92, 2012.
2. Wu CH, Chiu NC, Yeh YC, Kuo Y, Yu SS, Weng CY, Liu CA, Chou YH and Chiou YY: Uncommon liver tumors: Case report and literature review. Medicine (Baltimore) 95: e4952, 2016.
3. Folkman J: Angiogenesis. Annu Rev Med 57: 1-18, 2006.
4. Folkman J and Haudenschild C: Angiogenesis in vitro. Nature 288: 551-556, 1980.
5. Bry M, Kivelä R, Leppänen VM and Alitalo K: Vascular endothelial growth factor-B in physiology and disease. Physiol Rev 94: 779-794, 2014.
6. Folkman J: Tumor angiogenesis: Therapeutic implications. N Engl J Med 285: 1182-1186, 1971.
7. Dallas NA, Samuel S, Xia L, Fan F, Gray MJ, Lim SJ and Ellis LM: Endoglin (CD105): A marker of tumor vasculature and potential target for therapy. Clin Cancer Res 14: 1931-1937, 2008.

8. Cheifetz S, Bellón T, Calés C, Vera S, Bernabeu C, Massagué J and Letarte M: Endoglin is a component of the transforming growth factor-beta receptor system in human endothelial cells. J Biol Chem 267: 19027-19030, 1992.
9. López-Novoa JM and Bernabeu C: The physiological role of endoglin in the cardiovascular system. Am J Physiol Heart Circ Physiol 299: H959-H974, 2010.
10. Nagatsuka H, Hibi K, Gunduz M, Tsujigiwa H, Tamamura R, Sugahara T, Sasaki A and Nagai N: Various immunostaining patterns of CD31, CD34 and endoglin and their relationship with lymph node metastasis in oral squamous cell carcinomas. J Oral Pathol Med 34: 70-76, 2005.
11. Fonsatti E, Nicolay HJ, Altomonte M, Covre A and Maio M: Targeting cancer vasculature via endoglin/CD105: A novel antibody-based diagnostic and therapeutic strategy in solid tumours. Cardiovasc Res 86: 12-19, 2010.
12. Duff SE, Li C, Garland JM and Kumar S: CD105 is important for angiogenesis: Evidence and potential applications. FASEB J 17: 984-992, 2003.
13. Miller DW, Graulich W, Karges B, Stahl S, Ernst M, Ramaswamy A, Sedlacek HH, Müller R and Adamkiewicz J: Elevated expression of endoglin, a component of the TGF-beta-receptor complex, correlates with proliferation of tumor endothelial cells. Int J Cancer 81: 568-572, 1999.
14. Yang LY, Lu WQ, Huang GW and Wang W: Correlation between CD105 expression and postoperative recurrence and metastasis of hepatocellular carcinoma. BMC Cancer 6: 110, 2006.
15. Deshpande N, Needles A and Willmann JK: Molecular ultrasound imaging: Current status and future directions. Clin Radiol 65: 567-581, 2010.
16. Klibanov AL: Ligand-carrying gas-filled microbubbles: Ultrasound contrast agents for targeted molecular imaging. Bioconjug Chem 16: 9-17, 2005.
17. Abou-Elkacem L, Bachawal SV and Willmann JK: Ultrasound molecular imaging: Moving toward clinical translation. Eur J Radiol 84: 1685-1693, 2015.
18. Goodwin AP, Nakatsuka MA and Mattrey RF: Stimulus-responsive ultrasound contrast agents for clinical imaging: Motivations, demonstrations, and future directions. Wiley Interdiscip Rev Nanomed Nanobiotechnol 7: 111-123, 2015.
19. Schmitz G: Ultrasonic imaging of molecular targets. Basic Res Cardiol 103: 174-181, 2008.
20. Baron Toaldo M, Salvatore V, Marinelli S, Palamà C, Milazzo M, Croci L, Venerandi L, Cipone M, Bolondi L and Piscaglia F: Use of VEGFR-2 targeted ultrasound contrast agent for the early evaluation of response to sorafenib in a mouse model of hepatocellular carcinoma. Mol Imaging Biol 17: 29-37, 2015.
21. Streeter JE, Herrera-Loeza SG, Neel NF, Yeh JJ and Dayton PA. A comparative evaluation of ultrasound molecular imaging, perfusion imaging, and volume measurements in evaluating response to therapy in patient-derived xenografts. Technol Cancer Res Treat 12: 311-321, 2013.
22. Sirsi SR, Flexman ML, Vlachos F, Huang J, Hernandez SL, Kim HK, Johung TB, Gander JW, Reichstein AR, Lampl BS, *et al*: Contrast ultrasound imaging for identification of early responder tumor models to anti-angiogenic therapy. Ultrasound Med Biol 38: 1019-1029, 2012.
23. Anderson CR, Hu X, Zhang H, Tlaxca J, Declèves AE, Houghtaling R, Sharma K, Lawrence M, Ferrara KW and Rychak JJ: Ultrasound molecular imaging of tumor angiogenesis with an integrin targeted microbubble contrast agent. Invest Radiol 46: 215-224, 2011.
24. Deshpande N, Ren Y, Foygel K, Rosenberg J and Willmann JK: Tumor angiogenic marker expression levels during tumor growth: Longitudinal assessment with molecularly targeted microbubbles and US imaging. Radiology 258: 804-811, 2011.
25. Liu H, Chen Y, Yan F, Han X, Wu J, Liu X and Zheng H: Ultrasound molecular imaging of vascular endothelial growth factor receptor 2 expression for endometrial receptivity evaluation. Theranostics 5: 206-217, 2015.
26. Schmittgen TD and Livak KJ: Analyzing real-time PCR data by the comparative C(T) method. Nat Protoc 3: 1101-1108, 2008.
27. Zhang H, Li L, Wang Y, Dong F, Chen X, Liu F, Xu D, Yi F, Kapron CM and Liu J: NF-κB signaling maintains the survival of cadmium-exposed human renal glomerular endothelial cells. Int J Mol Med 38: 417-422, 2016.
28. Liu J, Kanki Y, Okada Y, Jin E, Yano K, Shih SC, Minami T and Aird WC: A +220 GATA motif mediates basal but not endotoxin-repressible expression of the von Willebrand factor promoter in Hprt-targeted transgenic mice. J Thromb Haemost 7: 1384-1392, 2009.
29. Zhu AX, Duda DG, Sahani DV and Jain RK: HCC and angiogenesis: Possible targets and future directions. Nat Rev Clin Oncol 8: 292-301, 2011.
30. Baek HJ, Lim SC, Kitisin K, Jogunoori W, Tang Y, Marshall MB, Mishra B, Kim TH, Cho KH, Kim SS and Mishra L: Hepatocellular cancer arises from loss of transforming growth factor beta signaling adaptor protein embryonic liver fodrin through abnormal angiogenesis. Hepatology 48: 1128-1137, 2008.
31. Grouls C, Hatting M, Rix A, Pochon S, Lederle W, Tardy I, Kuhl CK, Trautwein C, Kiessling F and Palmowski M: Liver dysplasia. US molecular imaging with targeted contrast agent enables early assessment. Radiology 267: 487-495, 2013.
32. Ferrante EA, Pickard JE, Rychak J, Klibanov A and Ley K: Dual targeting improves microbubble contrast agent adhesion to VCAM-1 and P-selectin under flow. J Control Release 140: 100-107, 2009.
33. Minhajat R, Mori D, Yamasaki F, Sugita Y, Satoh T and Tokunaga O: Endoglin (CD105) expression in angiogenesis of colon cancer: Analysis using tissue microarrays and comparison with other endothelial markers. Virchows Arch 448: 127-134, 2006.
34. Foygel K, Wang H, Machtaler S, Lutz AM, Chen R, Pysz M, Lowe AW, Tian L, Carrigan T, Brentnall TA and Willmann JK: Detection of pancreatic ductal adenocarcinoma in mice by ultrasound imaging of thymocyte differentiation antigen 1. Gastroenterology 145: 885-894.e3, 2013.
35. Tian H, Mythreye K, Golzio C, Katsanis N and Blobe GC: Endoglin mediates fibronectin/alpha5beta1 integrin and TGF-beta pathway crosstalk in endothelial cells. EMBO J 31: 3885-3900, 2012.
36. Park S, Sorenson CM and Sheibani N: PECAM-1 isoforms, eNOS and endoglin axis in regulation of angiogenesis. Clin Sci (Lond) 129: 217-234, 2015.
37. Bzyl J, Lederle W, Rix A, Grouls C, Tardy I, Pochon S, Siepmann M, Penzkofer T, Schneider M, Kiessling F and Palmowski M: Molecular and functional ultrasound imaging in differently aggressive breast cancer xenografts using two novel ultrasound contrast agents (BR55 and BR38). Eur Radiol 21: 1988-1995, 2011.